Differences in Immunoglobulin G Glycosylation Between Influenza and COVID-19 Patients

Kljaković-Gašpić Batinjan, Marina; Petrović, Tea; Vučković, Frano; Hadžibegović, Irzal; Radovani, Barbara; Jurin, Ivana; Đerek, Lovorka; Huljev, Eva; Markotić, Alemka; Lukšić, Ivica; ...

Source / Izvornik: **Engineering, 2023, 26, 54 - 62**

Journal article, Published version
Rad u časopisu, Objavljena verzija rada (izdavačev PDF)

https://doi.org/10.1016/j.eng.2022.08.007

Permanent link / Trajna poveznica: https://urn.nsk.hr/urn:nbn:hr:184:770239

Engineering 26 (2023) 54–62

Contents lists available at ScienceDirect

Engineering

journal homepage: www.elsevier.com/locate/eng

Research
Glycomedicine—Article

Differences in Immunoglobulin G Glycosylation Between Influenza and COVID-19 Patients

Marina Kljaković-Gašpić Batinjan [a,#], Tea Petrović [b,#], Frano Vučković [b], Irzal Hadžibegović [c,d], Barbara Radovani [e], Ivana Jurin [c], Lovorka Đerek [f], Eva Huljev [g], Alemka Markotić [h,i,j], Ivica Lukšić [k], Irena Trbojević-Akmačić [b], Gordan Lauc [b,l], Ivan Gudelj [b,e,*], Rok Čivljak [g,m]

[a] University Hospital Centre Zagreb, Zagreb 10000, Croatia
[b] Genos Glycoscience Research Laboratory, Zagreb 10000, Croatia
[c] Department of Cardiology, University Hospital Dubrava, Zagreb 10000, Croatia
[d] Faculty of Dental Medicine and Health, Josip Juraj Strossmayer University, Osijek 31000, Croatia
[e] Department of Biotechnology, University of Rijeka, Rijeka 51000, Croatia
[f] Department for Laboratory Diagnostics, University Hospital Dubrava, Zagreb 10000, Croatia
[g] Department for Acute Respiratory Infections, University Hospital for Infectious Diseases "Dr. Fran Mihaljević", Zagreb 10000, Croatia
[h] Department for Urogenital Infections, University Hospital for Infectious Diseases "Dr. Fran Mihaljević", Zagreb 10000, Croatia
[i] Department for Infectious Diseases, School of Medicine, Catholic University of Croatia, 10000 Zagreb, Croatia
[j] Postdoctoral Study, Faculty of Medicine, University of Rijeka, Rijeka 51000, Croatia
[k] Department of Maxillofacial Surgery, University of Zagreb School of Medicine, Dubrava University Hospital, Zagreb 10000, Croatia
[l] Faculty of Pharmacy and Biochemistry, University of Zagreb, Zagreb 10000, Croatia
[m] Department of Infectious Diseases, University of Zagreb School of Medicine, Zagreb 10000, Croatia

ARTICLE INFO

Article history:
Received 23 February 2022
Revised 1 August 2022
Accepted 13 August 2022
Available online 6 September 2022

Keywords:
Influenza
COVID-19
Viral infection
Glycosylation
Immunoglobulin G
Pneumonia

ABSTRACT

The essential role of immunoglobulin G (IgG) in immune system regulation and combatting infectious diseases cannot be fully recognized without an understanding of the changes in its *N*-glycans attached to the asparagine 297 of the fragment crystallizable (Fc) domain that occur under such circumstances. These glycans impact the antibody stability, half-life, secretion, immunogenicity, and effector functions. Therefore, in this study, we analyzed and compared the total IgG glycome—at the level of individual glycan structures and derived glycosylation traits (sialylation, galactosylation, fucosylation, and bisecting *N*-acetylglucosamine (GlcNAc))—of 64 patients with influenza, 77 patients with coronavirus disease 2019 (COVID-19), and 56 healthy controls. Our study revealed a significant decrease in IgG galactosylation, sialylation, and bisecting GlcNAc (where the latter shows the most significant decrease) in deceased COVID-19 patients, whereas IgG fucosylation was increased. On the other hand, IgG galactosylation remained stable in influenza patients and COVID-19 survivors. IgG glycosylation in influenza patients was more time-dependent: In the first seven days of the disease, sialylation increased and fucosylation and bisecting GlcNAc decreased; in the next 21 days, sialylation decreased and fucosylation increased (while bisecting GlcNAc remained stable). The similarity of IgG glycosylation changes in COVID-19 survivors and influenza patients may be the consequence of an adequate immune response to enveloped viruses, while the observed changes in deceased COVID-19 patients may indicate its deviation.

1. Introduction

Epidemics caused by respiratory viruses contribute significantly to the global health and socioeconomic burden and consequently affect the lives of millions of people [1,2]. Both severe acute respiratory syndrome coronavirus-2 (SARS-CoV-2) and influenza viruses can cause severe respiratory infections with significant

* Corresponding author.
E-mail address: ivan.gudelj@uniri.hr (I. Gudelj).
# These authors contributed equally to this work.

https://doi.org/10.1016/j.eng.2022.08.007

mortality [3]. However, mortality due to SARS-CoV-2 is strongly skewed toward people older than 70 years, unlike the 1918 and 2009 influenza pandemics [4]. Also, it has been observed that most coronavirus disease 2019 (COVID-19) patients with a severe form of the disease become critically ill 8–9 days after the onset of symptoms [5,6], which correlates with the time of activation of the adaptive immune response [7]. In this regard, antibodies can be considered a possible candidate of the adaptive immune system that could be responsible for the observed deterioration in the clinical course during SARS-CoV-2 infection.

Humoral immunity is required for the prevention of influenza infection through the neutralization of free infective particles [8,9]. One of the pivotal antibodies in this process is immunoglobulin G (IgG), which is the most abundant class of antibodies in the blood circulation [10]. The IgG molecule consists of two regions: the antigen-binding fragment (Fab) region and the fragment crystallizable (Fc) region. The Fab region is responsible for recognizing the antigens of various pathogens, while the Fc region has an effective function that determines the immune system response to the presence of pathogens. Within the Fc IgG region, there is a highly evolutionary conserved N-glycosylation site whose *N*-glycans affect antibody stability and modulate IgG effector functions [11–13]. Changes in Fc glycosylation can alter the Fc conformation and affect the binding to Fc receptors, both on the surface of innate immune cells and through interactions with the complement cascade [14–17]. Thus, core fucose removal from the *N*-glycan of the Fc region makes IgG 50-fold more effective in initiating antibody-dependent cellular cytotoxicity (ADCC) and consequently increases its antiviral activity [17,18]. Also, afucosylated antigen-specific IgG may be an important element in the defense against SARS-CoV-2 [19]. On the other hand, the fucosylation of anti-spike IgG negatively correlates with the macrophage production of proinflammatory cytokines interleukin-6 (IL-6) and IL-8, thereby promoting inflammation in patients with severe COVID-19 [20].

Interestingly, both SARS-CoV-2 and influenza viruses are enveloped viruses with glycoproteins on their membrane. Indeed, the immune responses to various enveloped viruses—but not to non-enveloped ones—exhibit one common finding: the afucosylation of antigen-specific IgG [5]. Similarly, afucosylated IgG has been found in people infected with human immunodeficiency virus (HIV) [21], dengue virus [22], cytomegalovirus (CMV), measles virus, mumps virus, hepatitis B virus, and SARS-CoV-2 [19], but not in cases of influenza virus. Interestingly, these changes were not observed after vaccination, indicating that the afucosylated IgG response requires membrane context [23]. Therefore, findings of IgG glycosylation alterations after vaccination cannot be directly transferred to glycosylation changes in natural infections, which further confirms the need to study glycosylation under different conditions. Therefore, the aim of this study was to perform in-depth profiling of the IgG *N*-glycans purified from adult patients infected with SARS-CoV-2 and influenza viruses using hydrophilic-interaction liquid chromatography–ultra-high-performance liquid chromatography (HILIC–UHPLC).

2. Materials and methods

2.1. Study population

2.1.1. Influenza patients

Sixty-four adult patients ($\geq$ 18 years of age) with laboratory-confirmed influenza were recruited during three consecutive winter seasons (2017/2018, 2018/2019, and 2019/2020) among patients hospitalized at the Department for Acute Respiratory Infection of the University Hospital for Infectious Diseases, Croatia, due to acute febrile illness. Blood samples for IgG isolation were collected at three time points, on the 1st, 7th, and 28th day after admission. Demographic, epidemiological, clinical, laboratory, microbiological, and other data regarding severity and outcome were also collected. The patients included in the study were hospitalized for acute febrile illness with or without respiratory symptoms lasting for $\leq$ 7 days, etiologically confirmed influenza with or without pneumonia, and laboratory-confirmed influenza in a naso/pharyngeal swab by single reverse transcription-polymerase chain reaction (RT-PCR). Patients excluded from the study included those younger than 18 years of age; patients treated with transfusions, intravenous immunoglobulins, or other blood derivatives in the past six months; and those who met one or more of the following criteria: acute febrile illness lasting for more than seven days, acute febrile illness without etiological evidence of influenza infection, etiologically confirmed other viral respiratory infection and/or bacterial co-infection, healthcare-associated infection, immunodeficiencies (e.g., malignant disease, chemotherapy, irradiation, solid organ and stem cell transplantation, asplenia, autoimmune disease, and immunosuppressive drugs), pregnancy, HIV infection, and tuberculosis.

2.1.2. COVID-19 patients

Seventy-seven adult patients with polymerase chain reaction (PCR)-confirmed SARS-CoV-2 infection from University Hospital Dubrava, Croatia, were included. University Hospital Dubrava was organized as a dedicated SARS-CoV-2 hospital from November 2020 to June 2021 and kept a prospective database of all patients hospitalized with SARS-CoV-2 with different levels of severity: ① mild: individuals with no evidence of pneumonia but with other important acute comorbidities; ② moderate: individuals with evidence of pneumonia, yet without a need for invasive mechanical ventilation; ③ severe: individuals with evidence of bilateral pneumonia, a need for admission to the hospital intensive care unit, and a need for invasive mechanical ventilation; and ④ critical: individuals with a need for immediate invasive mechanical ventilation and admission to the hospital intensive care unit, or a need for extracorporeal circulation, or deceased during hospitalization. This study included patients with mild, moderate, severe, and critical illness, in addition to clear evidence of SARS-CoV-2 infection that was the main reason for hospitalization. For this study, patients with moderate and severe illness were first merged into a single group and then later divided into two groups depending on survival (Table S1 in Appendix A). Blood was collected for plasma multiple times during hospitalization, and samples were collected between November and December 2020.

2.1.3. Healthy controls

This group included 56 volunteers recruited from the City of Zagreb and Zagreb County between June 2018 and February 2020 who were without clinical signs/symptoms or laboratory-suspected infectious disease and who were matched by age and sex to the patients. Blood samples for IgG isolation were collected on three occasions: on the 1st, 7th, and 28th day from inclusion in the study. Further characteristics of the study cohort are shown in Table 1.

For all samples, venous blood samples were collected in vacuum blood-collection tubes containing ethylenediaminetetraacetic acid (EDTA). The samples were allowed to rest for an hour and were then centrifuged at 1620*g* (1*g* = 9.8 $m \cdot s^{-2}$) for 10 min. Aliquots of plasma were then transferred to a 2 mL tube and centrifuged at 2700*g* for 10 min; after that, they were immediately stored at –20 °C until the analyses were performed.

Table 1
Study cohorts: number of samples and population characteristics.

Characteristics	Samples						
	2018		2019		2020		
	Influenza (n = 13)	Control (n = 35)	Influenza (n = 38)	Control (n = 0)	Influenza (n = 13)	Control (n = 21)	COVID-19 (n = 77)
Sex (male)	11	12	29	–	8	4	57
Age (year, median (IQR))	55 (51–69)	39 (32–51)	56(49–66)	–	41 (34–61)	77 (45–82)	72 (64–77)

2.2. IgG isolation, glycan release, and labeling

In brief, IgGs were isolated from the plasma samples using a protein G 96-well monolithic plate (BIA Separations, Slovenia) [24]. For the influenza patients and healthy controls, the isolated IgGs were denatured with the addition of sodium dodecyl sulfate (SDS) (Invitrogen, USA) and by incubation at 65 °C. The excess SDS was neutralized with Igepal-CA630 (Sigma-Aldrich, USA), and the *N*-glycans were released following the addition of PNGase F (Promega, USA) in phosphate-buffered saline (PBS). The released *N*-glycans were labeled with 2-aminobenzamide (2-AB). Free label and reducing agent were removed from the samples using hydrophilic-interaction liquid chromatography solid-phase extraction (HILIC-SPE). For the samples from the first two influenza seasons, a 0.2 μm AcroPrep GH Polypro (GHP) filter plate (Pall, USA) was used for the HILIC-SPE step; for the last season, an AcroPrep Advance 1 mL 0.2 μm wwPTFE plate (Pall) was used. Glycans were eluted with ultrapure water and stored at −20 °C until use.

For COVID-19 samples, glycan release, and labeling, a GlycoWorks RapiFluor-MS *N*-Glycan Kit (Waters, USA) was used. The protocol for this analysis has been described in detail by Deriš et al. [25]. In brief, dried IgG eluate (with an average mass of 15 μg) was resuspended in ultrapure water and 5% RapiGest SF solution (Waters). To denature the IgG, samples were incubated at 99 °C for 3 min. The *N*-glycans from the samples were enzymatically released from the proteins using GlycoWorks Rapid PNGase F (Waters) and incubated at 50 °C for 5 min. The released *N*-glycans were labeled with RapiFluor-MS Solution (Waters), and the plate was left at room temperature for 5 min. After labeling, the samples were mixed with acetonitrile (ACN; Honeywell, USA) and immediately transferred to a GlycoWorks HILIC μElution Plate (Waters) prior to the clean-up procedure by means of HILIC-SPE. The wells were prewashed with ultrapure water and ultrapure water/ACN (15:85, v/v) and then vacuumed to waste using a multi-well plate vacuum manifold (Pall). Glycans were eluted with 3× 30 μL of SPE Elution Buffer and 200 mmol·L^{-1} of ammonium acetate/ACN (95:5, v/v) at pH 7 (Waters), and then diluted with 310 μL of sample diluent, dimethylformamide (DMF)/ACN (32:68, v/v) (Waters). For each sample, 40 μL was transferred to a vial for HILIC–UHPLC analysis, while the remaining samples were stored at −20 °C.

2.3. HILIC–UHPLC analysis

Fluorescently labeled *N*-glycans were separated by means of HILIC on an Acquity UPLC instrument (Waters) consisting of a quaternary solvent manager, sample manager, and an fluorescence (FLR) detector. The instrument was under the control of Empower 3 software, build 3471 (Waters). Samples were maintained at 10 °C before injection, and the separation temperature was 60 °C. 2-AB-labeled *N*-glycans were separated on a Waters glycan ethylene bridged hybrid (BEH) amide chromatography column (100 mm × 2.1 mm; inner diameter (i.d.), 1.7 μm BEH particles), with 100 mmol·L^{-1} ammonium formate at pH 4.4 as solvent A and ACN as solvent B. The separation method used a linear gradient of 25%–38% solvent A (v/v) at a flow rate of 0.40 mL·min^{-1} in a 27-min analytical run. Excitation and emission wavelengths were set to 250 and 428 nm, respectively. The chromatograms were all separated in the same manner into 24 peaks, as previously reported [24].

RapiFluor-MS-labeled *N*-glycans were separated on a Waters glycan BEH amide chromatography column (100 mm × 2.1 mm; i.d., 1.7 μm BEH particles), with 50 mmol·L^{-1} ammonium formate at pH 4.4 as solvent A and ACN as solvent B. The separation method used a linear gradient of 75.0%–61.5% ACN (v/v) at a flow rate of 0.4 mL·min^{-1} in a 42-min analytical run. Excitation and emission wavelengths were set to 256 and 425 nm, respectively. The obtained chromatograms were separated into 22 peaks, regarding which the glycan structures have been described by Keser et al. [26].

In both cases, data processing was performed using an automatic processing method with a traditional integration algorithm, after which each chromatogram was manually corrected to maintain the same intervals of integration for all the samples. The amount of glycans in each peak was expressed as a percentage of the total integrated area.

2.4. Data analysis

Normalization and batch correction were performed on the UHPLC glycan data as described previously in order to remove experimental variation from the measurements. Depending on the fluorescent label used (i.e., 2-AB or RapiFluor-MS), the chromatograms were integrated into 24 or 22 directly measured glycan structures, and six derived traits were calculated from the directly measured glycans according to the following formulas:

- **For glycans labeled with 2-AB (GP):** For agalactosylated G0 = GP1 + GP2 + GP3 + GP4 + GP6, with one galactose G1 = GP7 + GP8 + GP9 + GP10 + GP11, with two galactoses G2 = GP12 + GP13 + GP14 + GP15, with a bisecting GlcNAc B = GP3 + GP6 + GP10 + GP11 + GP13 + GP15 + GP19 + GP22 + GP24, with a core fucose F = GP1 + GP4 + GP6 + GP8 + GP9 + GP10 + GP11 + GP14 + GP15 + GP16 + GP18 + GP19 + GP23 + GP24, and sialylated glycans S = GP16 + GP17 + GP18 + GP19 + GP20 + GP21 + GP22 + GP23 + GP24; for each derived trait, the obtained sum was divided by the sum of all the peaks and multiplied by 100.
- **For glycans labeled with RapiFluor-MS (RFGP):** For agalactosylated G0 = RFGP1 + RFGP2 + RFGP3 + RFGP4, with one galactose G1 = RFGP5 + RFGP6 + RFGP7 + RFGP8 + RFGP9 + RFGP10, with two galactoses G2 = RFGP11 + RFGP12 + RFGP13, with a bisecting GlcNAc B = RFGP4 + RFGP9 + RFGP10 + RFGP13 + RFGP17 + RFGP20 + RFGP22, with a core fucose F = RFGP1 + RFGP3 + RFGP4 + RFGP7 + RFGP8 + RFGP9 + RFGP10 + RFGP12 + RFGP13 + RFGP14 + RFGP16 + RFGP17 + RFGP21 + RFGP22, and sialylated glycans S = RFGP14 + RFGP15 + RFGP16 + RFGP17 + RFGP18 + RFGP19 + RFGP20 + RFGP21 + RFGP22; for each derived trait, the obtained sum was divided by the sum of all the peaks and multiplied by 100.

These derived traits average the particular glycosylation features across different individual glycan structures; consequently, they are closely related to individual enzymatic activities and underlying genetic polymorphisms.

A longitudinal analysis of the patient samples through their observation period was performed by implementing a linear

mixed-effects model in which glycan measurement was a dependent variable and time was modeled as a fixed effect; moreover, individual identification (ID) was included in a model as a random intercept, with age and gender included as additional covariates. For each cohort (i.e., healthy controls (C2018 and C2020) and patients with influenza (I2018, I2019, and I2020)), two longitudinal linear mixed model (LMM) analyses were performed: T1–T2 and T2–T3 analyses. Analyses were first performed for each cohort separately and then combined using a random-effects meta-analysis approach. Two separate meta-analyses were performed—one using the C2018 and C2020 results and another using the I2018, I2019, and I2020 results. Prior to the analyses, glycan variables were all transformed to a standard normal distribution (mean = 0, standard deviation (SD) = 1) by the inverse transformation of ranks to normality (*R* package "GenABEL," function rntransform). Using rank-transformed variables in the analyses made the estimated effects of different glycans in different cohorts comparable, as transformed glycan variables have the same standardized variance. The false discovery rate was controlled using the Benjamini–Hochberg procedure (function p.adjust(method = "BH")). Data was analyzed and visualized using *R* programming language (version 4.0.2).

3. Results

The PNGase F-released IgG *N*-glycans from 64 patients with influenza, 77 patients with COVID-19, and 56 healthy controls were fluorescently labeled and analyzed using HILIC–UHPLC. The obtained chromatograms were integrated into peaks, which mostly contained individual *N*-glycan structures (Fig. S1 in Appendix A) [24]. From the obtained peaks, derived glycan traits were calculated to represent the portion of structurally similar glycan structures that share common biosynthetic pathways. The statistical analysis was conducted only on the derived traits, and we did not observe any significant changes in the IgG glycome in the healthy controls (Figs. 1 and 2, and Figs. S2 and S3 and Table S2 in Appendix A).

3.1. Galactosylation

The derived traits that represent the level of galactosylation are G0 (all glycans without a galactose), G1 (all glycans with one galactose), and G2 (all glycans with two galactoses). The galactosylation of IgG seems to be very susceptible to COVID-19 (Fig. 1 and Table 2, and Table S3 in Appendix A). All the galactosylation-associated traits changed significantly in the COVID-19 patients, and these changes were dependent on COVID-19 mortality (Fig. 3 and Table 3, and Table S4 in Appendix A). Thus, G0 increased while G1 and G2 decreased in the deceased COVID-19 patients. In contrast, IgG galactosylation remained relatively stable in the COVID-19 survivors. Similarly, galactosylation stayed stable in the group of patients with influenza infection (only the increase of G1 between the second and third time points remained statistically significant after correction for multiple testing) (Fig. 2 and Table 4, and Fig. S3 and Table S5 in Appendix A).

3.2. Sialylation

Extensive and statistically significant changes in the addition of the terminal sialic acid to IgG *N*-glycans were observed in all groups of patients (Figs. 1 and 2). The presence of sialic acid in the IgG glycome steadily decreased in COVID-19 patients (Table 2 and Table S3 in Appendix A). However, during influenza infection, an increase in sialylation was observed between the first and second time point in all three analyzed seasons (this change did not reach statistical significance; see Fig. S3). Between the second and third time points, the proportion of sialylated glycan structures significantly decreased (Table 4 and Table S5).

3.3. Fucosylation

The presence of a core fucose changed extensively between all the time points in influenza patients. The level of core fucose decreased in the influenza patients between the first and second time points, but increased between the second and third time points (Fig. 2 and Table 4, and Fig. S4 and Table S5 in Appendix A). However, in the COVID-19 patients, fucosylation steadily increased with disease progression, and the increase was dependent on disease mortality (Figs. 1 and 3); the increase in fucosylation was more pronounced in the group of patients who died from COVID-19 (Fig. 3 and Table 3, and Table S4).

3.4. Presence of bisecting GlcNAc

Unlike fucosylation, the presence of bisecting GlcNAc significantly decreased in both diseases (Figs. 1 and 2). In the influenza patients, the decrease was statistically significant between the first and second time points, while the presence of bisecting GlcNAc remained stable between the second and third time points (Fig. 2 and Table 4, and Table S5). The decrease in the presence of bisecting GlcNAc was the most prominent change in IgG glycosylation in the COVID-19 patients, and was present regardless of the disease mortality (Figs. 1 and 3 and Table 3, and Table S4).

4. Discussion

In this study, we systematically examined IgG glycosylation changes in influenza infection during three seasons and compared them with changes observed in COVID-19 patients. This study is the first to explore IgG glycosylation differences between SARS-CoV-2 and influenza infections, and within influenza infection in general, with the aim of deepening our knowledge of the immune response to enveloped viruses. The most prominent IgG glycosylation feature associated with the immune response to enveloped viruses is core fucosylation. Although the absence of core fucosylation in IgG *N*-glycans has been known to increase ADCC for two decades [17], a decrease in core fucose level was just recently associated with the immune response to enveloped viruses and viral infection severity [19]. Thus, COVID-19 severity is associated with lower antigen-specific IgG fucosylation, while the total IgG fucosylation remains relatively stable [19]. Total IgG fucosylation stability in COVID-19 and its increase in more severe COVID-19 patients were observed in our study, as well as in a recently published study by Petrović et al. [27]. However, this is the first time that a decrease in IgG fucosylation during influenza infection has been observed at the level of total IgG, rather than only on antigen-specific IgG, as was recently suggested for enveloped viruses [19]. This brings our results closer to a recent study that associated the fucosylation level of both antigen-specific and total IgG with disease severity in secondary dengue infection [28]. Thus, these results indicate that—contrary to the abovementioned recently published study [19]—changes in fucosylation may also be observed on the total IgG for some enveloped viruses such as influenza and dengue virus. Therefore, these differences in IgG fucosylation are probably driven by different molecular mechanisms involved in the systematic immune response to different viral infections. Indeed, the cytokine milieu has been shown to differ between influenza and SARS-CoV-2 infections [29]. Influenza infection has been shown to trigger the release of myriad different cytokines, with interferon-α (IFNα) being one of the most prominent [30]. IFNα has already been

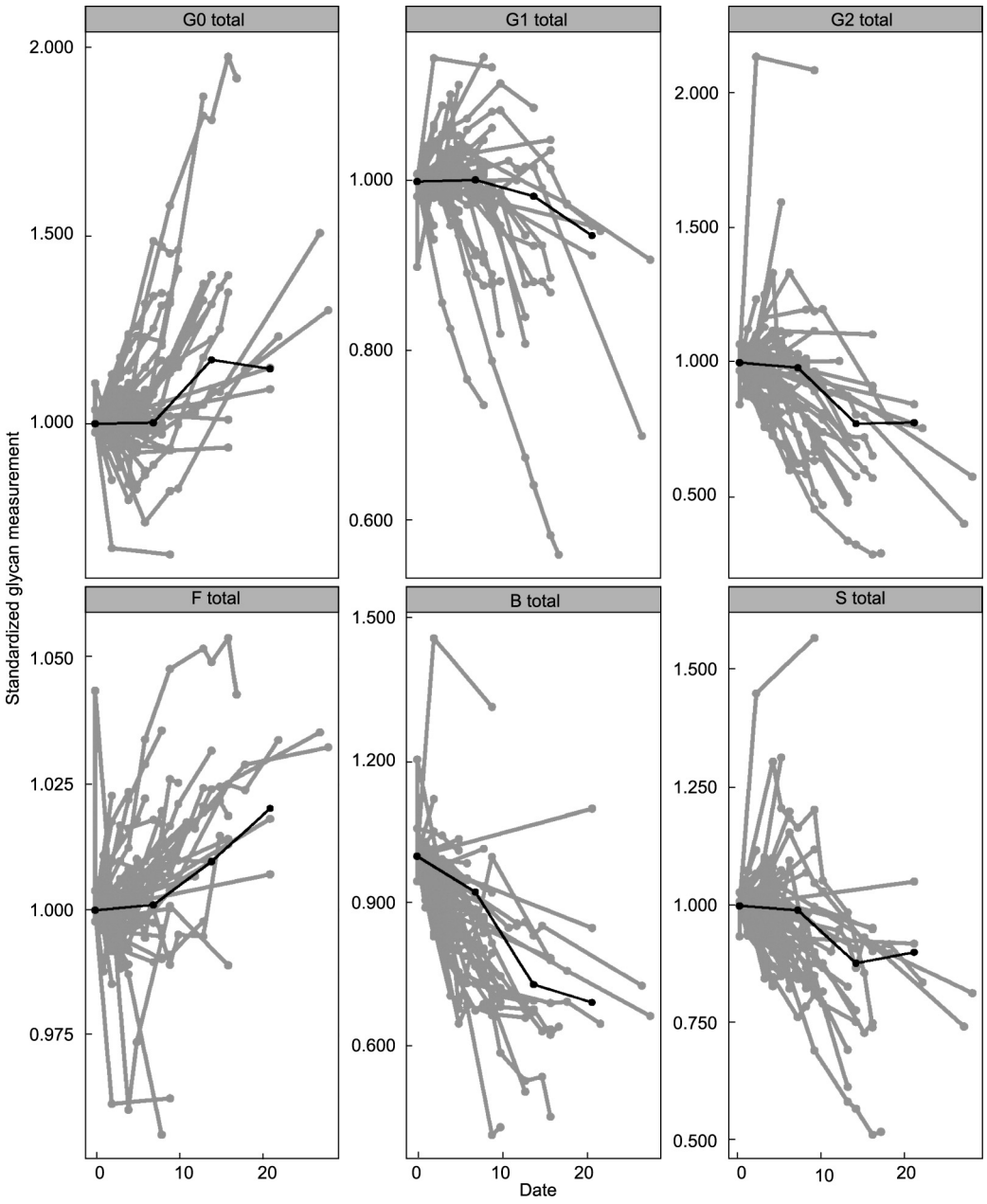

Fig. 1. IgG glycan composition changes during one season of COVID-19 normalized to the first point.

associated with the lower core fucosylation of IgG glycans, increasing IgG Fc affinity to Fcγ receptors, FcγRIIIA and FcγRIIIB, activating Fcγ receptors, consequently resulting in natural killer (NK) cell activation, and therefore significantly reinforcing ADCC [14,31]. On the other hand, it seems that the Type I and Type II IFN cascade is dysregulated in SARS-CoV-2 infections [29], which may potentially be a cause of an antigen-specific glycosylation regulation.

In contrast to fucosylation, galactosylation seems to be stable in influenza and COVID-19 survivors but significantly changed in deceased COVID-19 patients, resulting in a higher abundance of agalactosylated IgG molecules. The loss of galactose in the IgG N-glycome has already been associated with higher proinflammatory IgG function by triggering complement activation via the alternative pathway and/or the lectin pathway after binding to mannose-binding lectin [14]. However due to the high proportion of *N*-glycans without a core fucose during influenza infection, unchanged IgG galactosylation may act as a control mechanism, since it may initiate the anti-inflammatory signaling cascade through binding to the inhibitory receptor FcγRIIB [14].

Similarly, the presence of bisecting GlcNAc in the IgG glycome is associated with its proinflammatory activity [14] and was found to decrease in both of the infectious diseases studied here. In the COVID-19 patients, its decrease in the IgG glycome can be at least partially explained by the presence of the core fucose, which has an inhibitory effect on the addition of bisecting GlcNAc [32]. In contrast, in influenza infection, we observed a decrease in both core fucosylation and addition of bisecting GlcNAc in the IgG N-glycome, even though they were expected to shift in the opposite directions [14]. However, our observations—despite being hard to explain—are in accordance with the antigen-specific IgG glycosylation changes observed after influenza vaccination [33,34].

Moreover, an increase in sialylation in influenza patients between the first and second time point, albeit not statistically significant, is probably driven by the synthesis of antigen-specific IgG

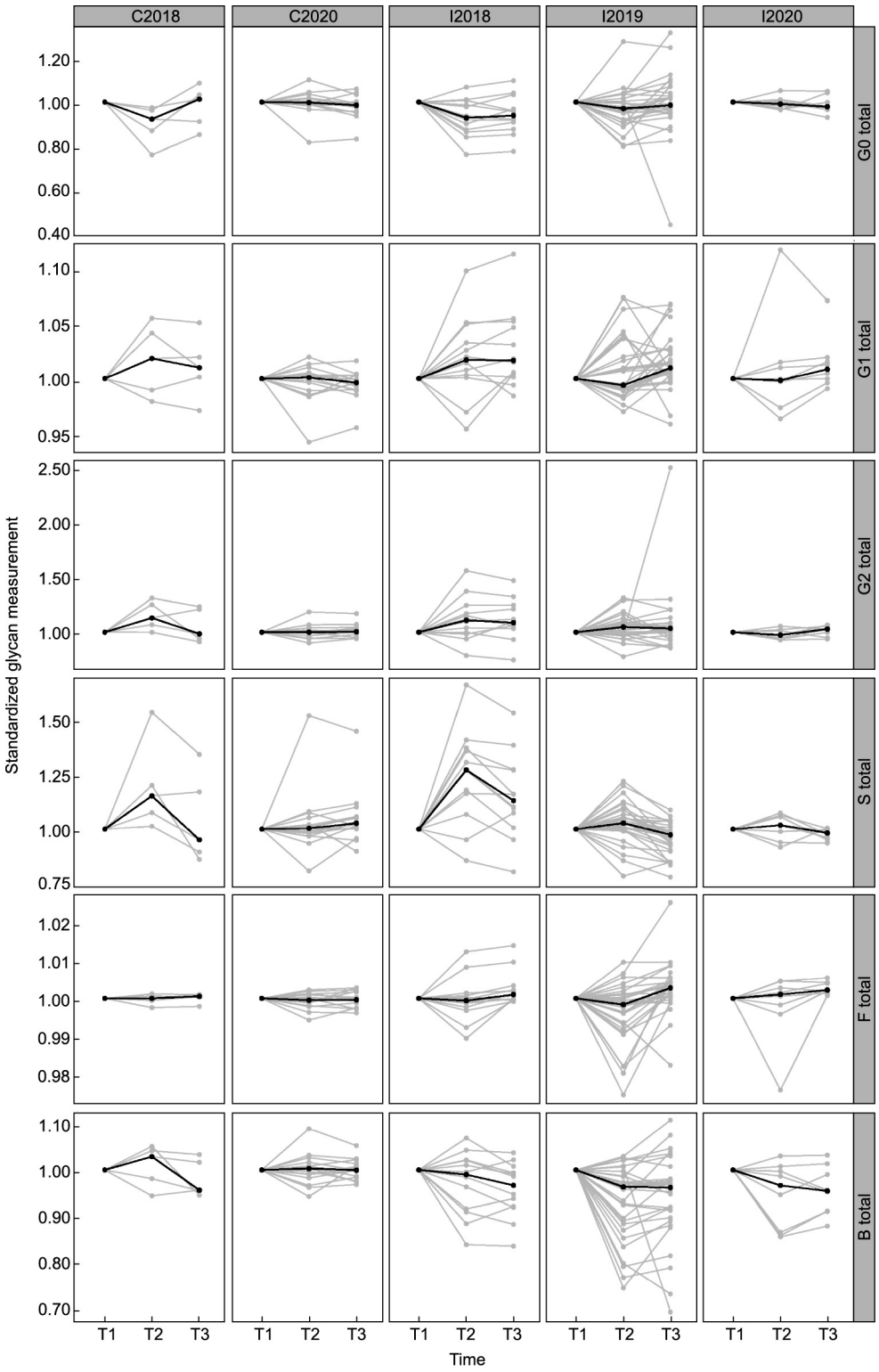

Fig. 2. IgG glycan composition changes during three seasons of influenza infection normalized to the first point. T: time point.

[33]. Those sialylated IgG antibodies are one of the factors influencing the quality of the response to an influenza antigen by binding to CD23, a Type II Fc receptor (C-type lectin), which elevates the expression of FcγRIIB, an inhibitory Type I Fc receptor, on activated B cells [33]. Furthermore, sialic acid is necessary for the successful attachment of the influenza virus to cells; therefore, increased sialylation of IgG's Fab region may block that attachment by mimicking sialylated receptors [35]. The initial increase in sialylation was followed by its decrease between the second and third time point in influenza disease, whereas it was found to continuously decrease in COVID-19 disease. This shift toward a more proinflammatory IgG glycome profile could be a consequence of an adaptive mechanism during prolonged infection through the activation of Type I Fcγ receptors [14,33]. In the case of influenza, it could also

Table 2
Association of COVID-19 disease with changes in IgG N-glycome-derived traits.

Glycan trait	Effect[a]	Standard error	*P* value	Adjusted *P* value[b]
G0	0.0504	0.0120	0.0002	0.0003
G1	−0.0320	0.0128	0.0195	0.0195
G2	−0.0546	0.0128	0.0001	0.0003
F	0.0459	0.0105	0.0001	0.0003
B	−0.0857	0.0092	2.4×10^{-13}	1.4×10^{-12}
S	−0.0433	0.0109	0.0005	0.0006

[a] Effect: model coefficient (slope) representing the change in a glycan trait (expressed in SD units) per unit of time.
[b] Adjustment for multiple testing using the Benjamini–Hochberg procedure.

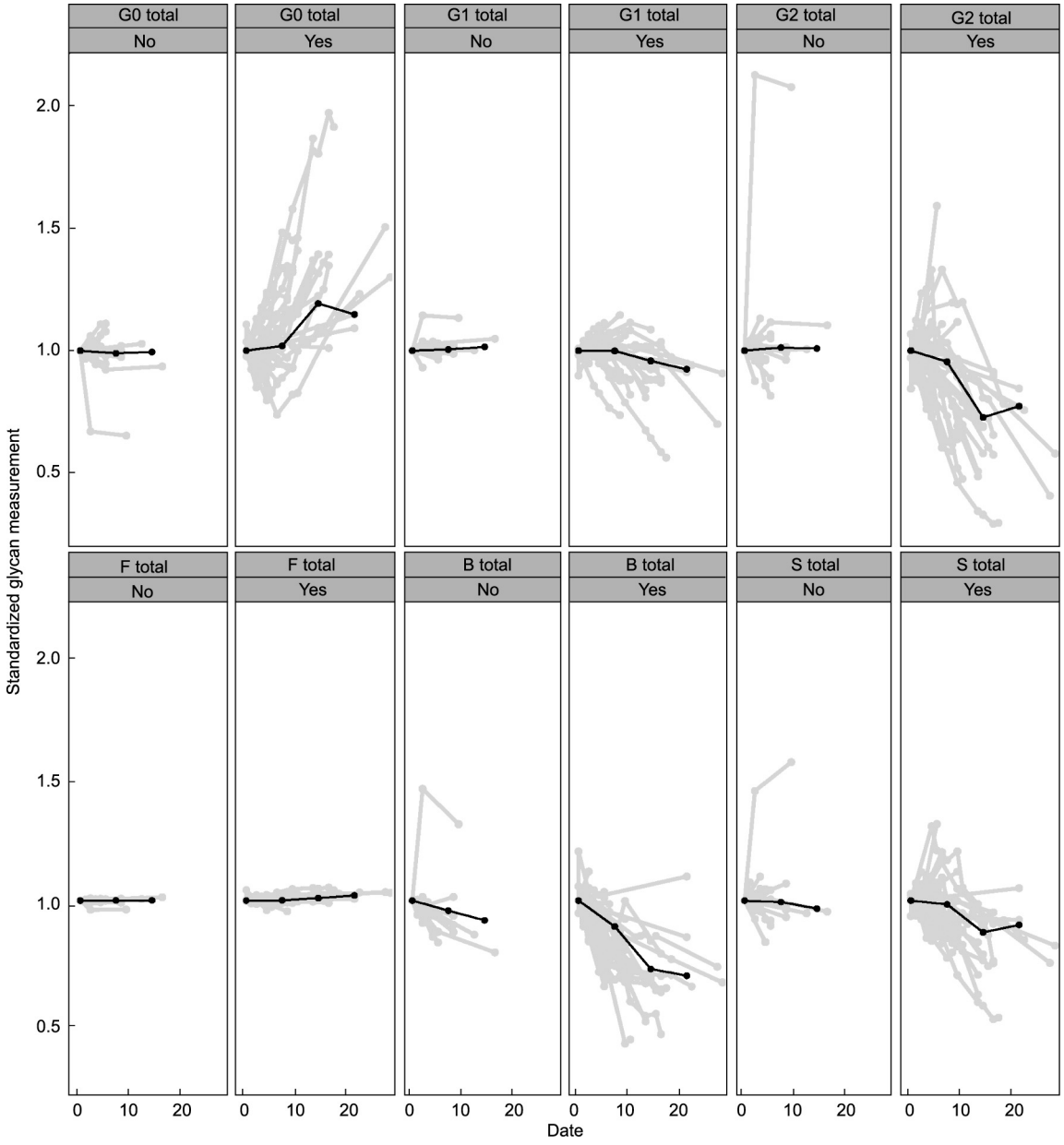

Fig. 3. IgG glycan composition changes in COVID-19 survivors (No) and deceased COVID-19 patients (Yes).

be the result of a shift in IgG production from plasmablasts to memory B cells, as has been observed three weeks after influenza vaccination [33].

Taken together, these IgG glycome alterations show that IgG glycosylation is a dynamic and strictly regulated process that enables fine-tuning of the immune response to a specific pathogen. Thus, in influenza infection, it can be regulated in a manner that increases cellular toxicity by lowering its fucosylation, while higher sialylation can neutralize virus infection and promote the production of high-affinity and broadly neutralizing IgGs. On the other hand, this study shows that the total IgG glycome is prone to changes during COVID-19 infection and that those glycome

Table 3
Association of COVID-19 mortality with changes in IgG N-glycome-derived traits.

Glycan trait	Effect[a]	Standard error	*P* value	Adjusted *P* value[b]
G0	0.0774	0.0237	0.0025	0.0038
G1	−0.0845	0.0263	0.0023	0.0038
G2	−0.0839	0.0247	0.0016	0.0038
F	0.0704	0.0223	0.0025	0.0038
B	−0.0371	0.0200	0.0676	0.0677
S	−0.0467	0.0231	0.0558	0.0669

[a] Effect: difference between two model coefficients (slopes), where each coefficient represents the group-specific change in the glycan trait (expressed in SD units) per unit of time.
[b] Adjustment for multiple testing using the Benjamini–Hochberg procedure.

Table 4
Association of influenza disease with changes in IgG N-glycome-derived traits between three time points.

Glycan trait	Time	Effect[a]	Standard error	*P* value	Adjusted *P* value[b]
G0	T1–T2	−0.1534	0.0919	0.0950	0.2012
	T2–T3	0.0555	0.0726	0.4446	0.6402
G1	T1–T2	0.1388	0.0594	0.0195	0.0502
	T2–T3	0.1707	0.0674	0.0113	0.0314
G2	T1–T2	0.1223	0.0769	0.1120	0.2123
	T2–T3	0.0695	0.0620	0.2626	0.4491
S	T1–T2	0.2952	0.1687	0.0801	0.1803
	T2–T3	−0.4720	0.0681	4.2×10^{-12}	5.0×10^{-11}
F	T1–T2	−0.2266	0.0707	0.0013	0.0049
	T2–T3	0.4932	0.0768	1.3×10^{-10}	1.2×10^{-9}
B	T1–T2	−0.3693	0.0627	3.8×10^{-9}	2.7×10^{-8}
	T2–T3	0.0006	0.0637	0.9926	0.9926

[a] Effect: model coefficient (slope) representing the change in a glycan trait (expressed in SD units) per unit of time.
[b] Adjustment for multiple testing using the Benjamini–Hochberg procedure.

alterations are not necessarily the same as those observed in antigen-specific IgG. Also, some IgG glycosylation traits in COVID-19, such as fucosylation, do not follow the IgG glycosylation pattern observed in influenza patients. However, there was a higher overlap in IgG glycosylation dynamics between influenza patients and COVID-19 survivors than between the former and deceased COVID-19 patients, which exhibited a more pronounced proinflammatory character of IgG glycosylation. This finding may be an indicator that the immune response in COVID-19 survivors is somewhat similar to the general immune response to other enveloped viruses, whereas the immune response in deceased COVID-19 patients becomes more deviant. Therefore, these differences may be used as a potential biomarker of an abnormal immune response during viral infections. Nevertheless, further experiments are needed to completely illuminate the molecular mechanisms behind the glycosylation changes observed in this study.

Acknowledgments

This work was supported by the European Structural and Investment Funds grant for the Croatian National Centre of Competence in Molecular Diagnostics (KK.01.2.2.03.0006); and the Croatian National Centre of Research Excellence in Personalized Healthcare grant (KK.01.1.1.01.0010). This work was also supported by the Human Glycome Project. Equipment and products from Waters and New England Biolabs®, Inc., were used for this research.

Compliance with ethics guidelines

The authors declare the following financial interests/personal relationships, which may be considered as potential competing interests: Gordan Lauc is the founder and owner, and Tea Petrović, Frano Vučković, Irena Trbojević-Akmačić, and Ivan Gudelj are employees of Genos Ltd., a company that specializes in high-throughput glycomics and has several patents in this field. The remaining authors declare that the research was conducted in the absence of any commercial or financial relationships that could be construed as a potential conflict of interest. The study was approved by the Ethics Committee of the University Hospital Dubrava and the University Hospital for Infectious Diseases (Ref. No. 01-1490-2-2017), Croatia, and performed in accordance with the *Declaration of Helsinki*. The patients and healthy controls were informed about the purpose of the study and gave their written informed consent.

Appendix A. Supplementary data

Supplementary data to this article can be found online at https://doi.org/10.1016/j.eng.2022.08.007.

References

[1] Szucs T. The socio-economic burden of influenza. J Antimicrob Chemother 1999;44(Suppl B):11–5.
[2] Suthar S, Das S, Nagpure A, Madhurantakam C, Tiwari SB, Gahlot P, et al. Epidemiology and diagnosis, environmental resources quality and socio-economic perspectives for COVID-19 pandemic. J Environ Manage 2021;280:111700.
[3] Piroth L, Cottenet J, Mariet AS, Bonniaud P, Blot M, Tubert-Bitter P, et al. Comparison of the characteristics, morbidity, and mortality of COVID-19 and seasonal influenza: a nationwide, population-based retrospective cohort study. Lancet Respir Med 2021;9(3):251–9.
[4] Petersen E, Koopmans M, Go U, Hamer DH, Petrosillo N, Castelli F, et al. Comparing SARS-CoV-2 with SARS-CoV and influenza pandemics. Lancet Infect Dis 2020;20(9):e238–44.
[5] Wang D, Hu B, Hu C, Zhu F, Liu X, Zhang J, et al. Clinical characteristics of 138 hospitalized patients with 2019 novel coronavirus-infected pneumonia. JAMA 2020;323(11):1061–9.
[6] Huang C, Wang Y, Li X, Ren L, Zhao J, Hu Y, et al. Clinical features of patients infected with 2019 novel coronavirus. Lancet 2020;395(10223):497–506.
[7] Thevarajan I, Nguyen THO, Koutsakos M, Druce J, Caly L, van de Sandt CE, et al. Breadth of concomitant immune responses prior to patient recovery: a case report of non-severe COVID-19. Nat Med 2020;26(4):453–5.

[8] Wrammert J, Koutsonanos D, Li GM, Edupuganti S, Sui J, Morrissey M, et al. Broadly cross-reactive antibodies dominate the human B cell response against 2009 pandemic H1N1 influenza virus infection. J Exp Med 2011;208(1):181–93.
[9] Chiu C, Ellebedy AH, Wrammert J, Ahmed R. B cell responses to influenza infection and vaccination. Curr Top Microbiol Immunol 2015;386:381–98.
[10] Plebani A, Ugazio AG, Avanzini MA, Massimi P, Zonta L, Monafo V, et al. Serum IgG subclass concentrations in healthy subjects at different age: age normal percentile charts. Eur J Pediatr 1989;149(3):164–7.
[11] Gornik O, Pavić T, Lauc G. Alternative glycosylation modulates function of IgG and other proteins—implications on evolution and disease. Biochim Biophys Acta 2012;1820(9):1318–26.
[12] Vidarsson G, Dekkers G, Rispens T. IgG subclasses and allotypes: from structure to effector functions. Front Immunol 2014;5:520.
[13] Kobata A. The N-linked sugar chains of human immunoglobulin G: their unique pattern, and their functional roles. Biochim Biophys Acta 2008;1780(3):472–8.
[14] Gudelj I, Lauc G, Pezer M. Immunoglobulin G glycosylation in aging and diseases. Cell Immunol 2018;333:65–79.
[15] Lux A, Yu X, Scanlan CN, Nimmerjahn F. Impact of immune complex size and glycosylation on IgG binding to human FcγRs. J Immunol 2013;190(8):4315–23.
[16] Czajkowsky DM, Andersen JT, Fuchs A, Wilson TJ, Mekhaiel D, Colonna M, et al. Developing the IVIG biomimetic, hexa-Fc, for drug and vaccine applications. Sci Rep 2015;5(1):9256.
[17] Shields RL, Lai J, Keck R, O'Connell LY, Hong K, Meng YG, et al. Lack of fucose on human IgG1 N-linked oligosaccharide improves binding to human FcγRIII and antibody-dependent cellular toxicity. J Biol Chem 2002;277(30):26733–40.
[18] Forthal DN, Gach JS, Landucci G, Jez J, Strasser R, Kunert R, et al. Fc-glycosylation influences Fcγ receptor binding and cell-mediated anti-HIV activity of monoclonal antibody 2G12. J Immunol 2010;185(11):6876–82.
[19] Larsen MD, de Graaf EL, Sonneveld ME, Plomp HR, Nouta J, Hoepel W, et al. Afucosylated IgG characterizes enveloped viral responses and correlates with COVID-19 severity. Science 2021;371(6532):eabc8378.
[20] Hoepel W, Chen HJ, Geyer CE, Allahverdiyeva S, Manz XD, de Taeye SW, et al. High titers and low fucosylation of early human anti-SARS-CoV-2 IgG promote inflammation by alveolar macrophages. Sci Transl Med 2021;13(596):eabf8654.
[21] Ackerman ME, Crispin M, Yu X, Baruah K, Boesch AW, Harvey DJ, et al. Natural variation in Fc glycosylation of HIV-specific antibodies impacts antiviral activity. J Clin Invest 2013;123(5):2183–92.
[22] Wang TT, Sewatanon J, Memoli MJ, Wrammert J, Bournazos S, Bhaumik SK, et al. IgG antibodies to dengue enhanced for FcγRIIIA binding determine disease severity. Science 2017;355(6323):395–8.
[23] Larsen MD, de Graaf EL, Sonneveld ME, Plomp HR, Nouta J, Hoepel W, et al. Afucosylated IgG characterizes enveloped viral responses and correlates with COVID-19 severity. Science 2021;371(6532):eabc8378.
[24] Pucić M, Knezević A, Vidič J, Adamczyk B, Novokmet M, Polašek O, et al. High throughput isolation and glycosylation analysis of IgG-variability and heritability of the IgG glycome in three isolated human populations. Mol Cell Proteomics 2011;10(10):010090.
[25] Deriš H, Cindrić A, Lauber M, Petrović T, Bielik A, Taron CH, et al. Robustness and repeatability of GlycoWorks RapiFluor-MS IgG *N*-glycan profiling in a long-term high-throughput glycomic study. Glycobiology 2021;31(9):1062–7.
[26] Keser T, Pavić T, Lauc G, Gornik O. Comparison of 2-aminobenzamide, procainamide and RapiFluor-MS as derivatizing agents for high-throughput HILIC-UPLC-FLR-MS *N*-glycan analysis. Front Chem 2018;6:324.
[27] Petrović T, Alves I, Bugada D, Pascual J, Vučković F, Skelin A, et al. Composition of the immunoglobulin G glycome associates with the severity of COVID-19. Glycobiology 2021;31(4):372–7.
[28] Bournazos S, Vo HTM, Duong V, Auerswald H, Ly S, Sakuntabhai A, et al. Antibody fucosylation predicts disease severity in secondary dengue infection. Science 2021;372(6546):1102–5.
[29] Olbei M, Hautefort I, Modos D, Treveil A, Poletti M, Gul L, et al. SARS-CoV-2 causes a different cytokine response compared to other cytokine storm-causing respiratory viruses in severely Ill patients. Front Immunol 2021;12:629193.
[30] Liu Q, Zhou YH, Yang ZQ. The cytokine storm of severe influenza and development of immunomodulatory therapy. Cell Mol Immunol 2016;13(1):3–10.
[31] Giron LB, Colomb F, Papasavvas E, Azzoni L, Yin X, Fair M, et al. Interferon-α alters host glycosylation machinery during treated HIV infection. EBioMedicine 2020;59:102945.
[32] Kurimoto A, Kitazume S, Kizuka Y, Nakajima K, Oka R, Fujinawa R, et al. The absence of core fucose up-regulates GnT-III and Wnt target genes: a possible mechanism for an adaptive response in terms of glycan function. J Biol Chem 2014;289(17):11704–14.
[33] Wang T, Maamary J, Tan G, Bournazos S, Davis C, Krammer F, et al. Anti-HA glycoforms drive B cell affinity selection and determine influenza vaccine efficacy. Cell 2015;162(1):160–9.
[34] Irvine EB, Alter G. Understanding the role of antibody glycosylation through the lens of severe viral and bacterial diseases. Glycobiology 2020;30(4):241–53.
[35] Huang T, Chen X, Zhao C, Liu X, Zhang Z, Li T, et al. Sialylated immunoglobulin G can neutralize influenza virus infection through receptor mimicry. Oncotarget 2016;7(13):15606–17.